

# Thermal characteristics of a B8.3 flare observed on July 04, 2009

Arun Kumar Awasthi<sup>1</sup>, Barbara Sylwester<sup>2</sup>, Janusz Sylwester<sup>2</sup> and  
Rajmal Jain<sup>3</sup>

<sup>1</sup>Astronomical Institute, University of Wrocław, Poland  
email: arun.awasthi.87@gmail.com

<sup>2</sup>Space Research Center of Polish Academy of Sciences, Wrocław, Poland  
email: bs@cbk.pan.wroc.pl, js@cbk.pan.wroc.pl

<sup>3</sup>Kadi Sarva Vishwavidyalaya, Gandhinagar, India  
email: rajmal\_9@yahoo.com

**Abstract.** We explore the temporal evolution of flare plasma parameters including temperature ( $T$ ) - differential emission measure ( $DEM$ ) relationship by analyzing high spectral and temporal cadence of X-ray emission in 1.6-8.0 keV energy band, recorded by SphinX (Polish) and Solar X-ray Spectrometer (SOXS; Indian) instruments, during a B8.3 flare which occurred on July 04, 2009. SphinX records X-ray emission in 1.2-15.0 keV energy band with the temporal and spectral cadence as good as 6  $\mu$ s and 0.4 keV, respectively. On the other hand, SOXS provides X-ray observations in 4-25 keV energy band with the temporal and spectral resolution of 3 s and 0.7 keV, respectively. We derive the thermal plasma parameters during impulsive phase of the flare employing well-established Withbroe-Sylwester DEM inversion algorithm.

**Keywords.** Sun: corona, Sun: flares, plasmas, Sun: X-rays, radiation mechanisms: thermal, techniques: spectroscopic.

---

## 1. Introduction

Thermal characteristics of solar flare plasma employing the multi-wavelength observations is of immense interest as it can shed light on the ongoing coupling processes in solar atmosphere. In particular, X-ray emission during a flare is the best probe of various thermal and non-thermal energy release processes (Brown (1971)). Generally, flare plasma parameters viz. temperature ( $T$ ), emission measure ( $EM$ ), etc. are derived by forward-fitting/inversion of the observed X-ray spectrum (Jain *et al.* (2011)). However, the spectroscopic inversion of X-ray emission is an ill-posed problem, leading to substantial uncertainties in the derived  $T$  and  $EM$  values (Craig & Brown (1976)). Moreover, several different  $DEM$  inversion techniques, with various functional dependence of  $DEM$  on  $T$  viz. power-law, single-gaussian etc., are used to interpret observed X-ray spectrum. Further, Withbroe-Sylwester (W-S)  $DEM$  inversion algorithm (Sylwester, Schrijver, & Mewe (1980), Kepa *et al.* (2008)) provides a more general scheme for such studies.

Therefore, in this paper, we present the analysis of X-ray emission observed during a B8.3 flare occurred on July 04, 2009, the only event recorded in common with Solar X-ray Spectrometer (SOXS; Jain *et al.* (2005)) and Solar Photometer in X-rays (SphinX; Gburek *et al.* (2013)). Section 2 presents the observations while data analysis and results are given in Section 3. Section 4 presents the summary and conclusions.

## 2. Observations

We study a B8.3 flare event of July 04, 2009, which occurred in active region 11024. Thermal characteristics of the flare plasma are derived by analyzing X-ray spectra in 1.6-5.0 keV and 5.0-8.0 keV energy bands, recorded by SphinX and SOXS, respectively. Temporal evolution of X-ray emission during the flare as observed by SphinX and SOXS instruments as well as by *GOES* is shown in the left panel of the Fig. 1. Further, morphological evolution of the flaring region is studied from the EUV images obtained from *STEREO-A*, *B* and Extreme Ultraviolet Imager Telescope (EIT) onboard *SOHO* mission, as shown in the right panel of the Fig. 1.

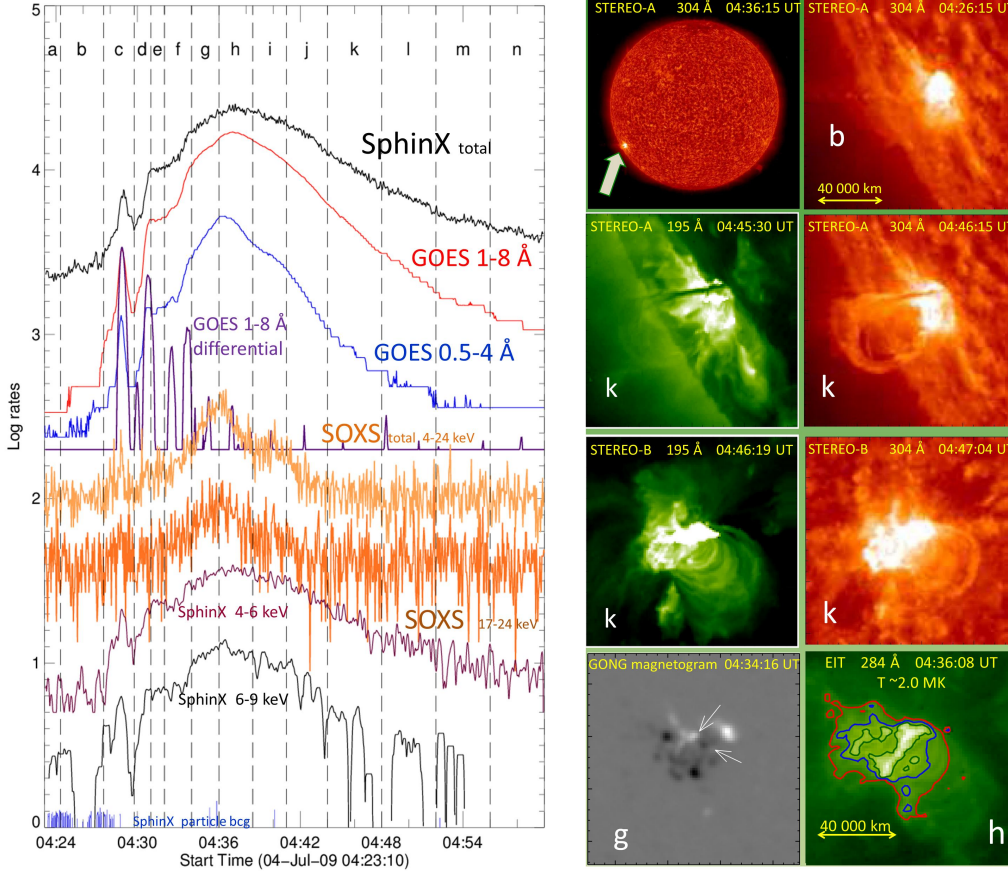


**Figure 1.** Left Panel: Temporal evolution of X-ray emission as recorded by SphinX, SOXS and *GOES* during SOL2009-07-04T04:37 (B8.3) flare. Dotted bars show the time intervals for which spectral analysis is undertaken. Right Panel: Multi-wavelength overview of the flare from *STEREO-A* and *STEREO-B* and EIT/*SOHO*. Activity areas are shown by arrows in the GONG Magnetogram (bottom).

## 3. Thermal characteristics of the flare plasma

We analyze the X-ray spectra, recorded during the flare, with the help of *W-S DEM* inversion method (Sylwester, Schrijver, & Mewe (1980)). This numerical method employs maximum likelihood approach in which a *DEM-T* distribution and hence corresponding

theoretical spectrum is derived in an iterative manner with the aim to minimize its difference with the input observed spectrum (Kepa *et al.* (2008)). Coronal abundances are adopted from CHIANTI atomic database (Del Zanna *et al.* (2015)) while deriving the shape of theoretical spectra. As an input to this method, we have used fluxes recorded in the 73 energy bins (corresponding to the energy band 1.6-5.0 keV) and 35 energy bins (corresponding to the energy band 5.0-8.0 keV) by SphinX and SOXS instruments, respectively. The X-ray spectra are analyzed for various time duration as shown by dotted lines in the left panel of Fig. 1. Top row of the Fig. 2 shows the best-fit  $DEM - T$  relation derived by analyzing X-ray spectrum in 1.6-5.0 keV (low-energy), observed by SphinX during the peak of the impulsive phase of the flare, 04:36:00-04:38:30 UT. Similarly, in the bottom panel, we present the best-fit  $DEM - T$  curve and spectral-fit over the X-ray spectrum in 5.0-8.0 keV (high-energy), observed by SOXS during the aforesaid time.

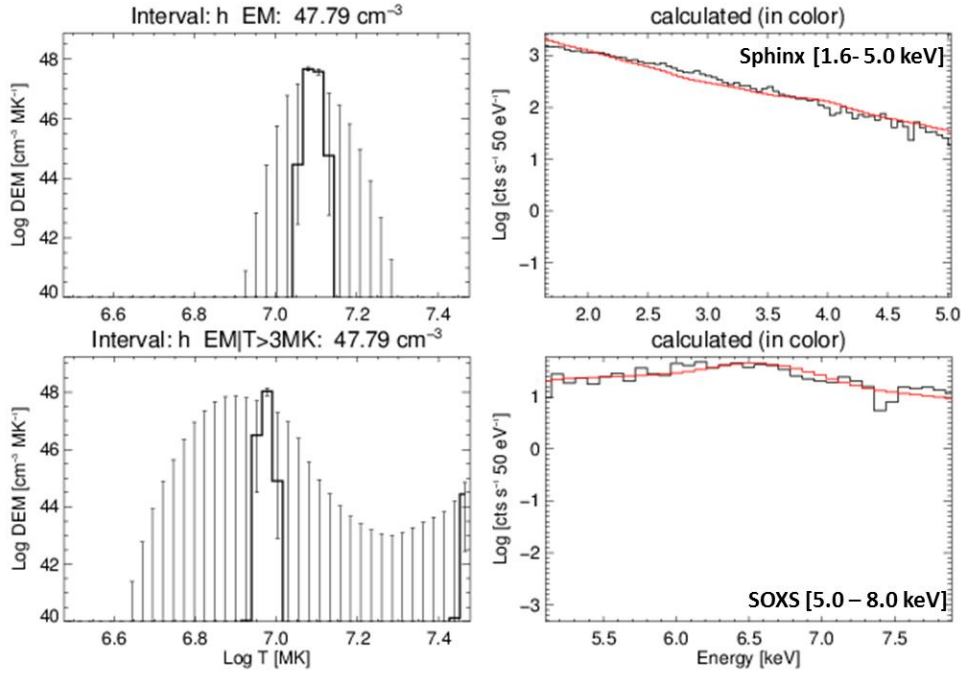


**Figure 2.** Top row: Best-fit  $DEM - T$  relationship as well as the spectral-fit (drawn by red color) employing W-S inversion algorithm for the emission in 1.6-5.0 keV (plotted by black color), recorded by SphinX during 04:36:00-04:38:30 UT. Bottom row: Best-fit  $DEM - T$  and fitted SOXS spectrum in 5.0 - 8.0 keV for the aforesaid time duration.

From Fig. 2, it may be noted that the best-fit  $DEM - T$  relation derived from SphinX observation suggests nearly isothermal nature of the  $DEM$ , with the peak at temperature ( $T_p$ )  $\sim 13$  MK. Similarly, the best-fit  $DEM$  to the SOXS spectrum in 5.0-8.0 keV energy band for the same time interval suggests isothermal nature in the form of single gaussian function dependence on  $T$ , however, at  $T_p = 9.8$  MK. Next, thermal energy are derived from the best-fit  $DEM - T$  curve of SphinX and SOXS observations and estimated to be  $5.1$  and  $3.6 \times 10^{29}$  ergs, respectively. We employ the volume estimated from EIT/SOHO EUV wavelength images as shown in Fig. 1 for the calculation of thermal energies.

#### 4. Summary and Conclusions

We study the thermal characteristics of the plasma during SOL2009-07-04T04:37 (B8.3) flare by analyzing its X-ray spectrum in various energy bands, as obtained by SphinX and SOXS instruments. We summarize the preliminary findings of this study as follows:

(a) Emission-measure is found to be of isothermal nature during the peak of the impulsive phase of the flare.

(b) Thermal energy and the temperature estimated by analyzing low-energy (from SphinX) and high-energy (from SOXS) bands within SXR spectrum result in different peak temperature as well as thermal energy.

In the next step, we have made a detailed investigation of thermal characteristics as well as the evolution of *DEM-T* relationship in various phases of the flare by combining the observations from SphinX and SOXS instruments (Awasthi et al. (2016)).

**Acknowledgements:** This research has been supported by Polish grant UMO-2011/01/M/ST9/06096. Moreover, the research leading to these results has received funding from the European Community's Seventh Framework Programme (FP7/2007-2013) under grant agreement no. 606862 (F-CHROMA).

#### References

- Awasthi, A.K., Sylwester, B., Sylwester, J. & Jain, R. 2016, *Accpeted for publication in the ApJ*
- Brown, J.C. 1971, *Solar Phys.*, 18, 489.
- Craig, I.J.D. & Brown, J.C. 1976, *A & A*, 49, 239.
- Del Zanna, G., Dere, K.P., Young, P.R., Landi, E., & Mason, H.E. 2015, *A & A*, 582, A56
- Gburek, S., Sylwester, J., Kowalinski, M., Bakala, J., Kordylewski, Z., Podgorski, P., Plocieniak, S., Siarkowski, M., Sylwester, B., Trzebinski, W., Kuzin, S.V., Pertsov, A.A., Kotov, Y.D., Farnik, F., Reale, F., & Phillips, K.J.H. 2013, *Solar Phys.*, 283, 631.
- Jain, R., Awasthi, A.K., Rajpurohit, A.S., & Aschwanden, M.J. 2011, *Solar Phys.*, 270, 137.
- Jain, R., Dave, H., Shah, A.B., Vadher, N.M., Shah, V.M., Ubale, G.P., Manian, K.S.B., Solanki, C.M., Shah, K.J., Kumar, S., Kayasth, S.L., Patel, V.D., Trivedi, J.J., & Deshpande, M.R. 2005, *Solar Phys.*, 227, 89.
- Kepa, A., Sylwester, B., Siarkowski, M., & Sylwester, J. 2008, *Adv. Sp. Res.*, 42, 828.
- Sylwester, J., Schrijver, J., & Mewe, R. 1980, *Solar Phys.*, 67, 285